



Forest gradient response in Sierran landscapes: the physical template

Dean L. Urban^{1,*}, Carol Miller^{2,*}, Patrick N. Halpin¹ & Nathan L. Stephenson³

¹Nicholas School of the Environment, Duke University, Durham, NC 27708 USA; ²Graduate Degree Program in Ecology, Colorado State University, Fort Collins, CO 80523, USA; ³US Geological Survey, Biological Resources Division, Sequoia-Kings Canyon Field Station, Three Rivers, CA 93271, USA; **Present address: Aldo Leopold Wilderness Research Institute, USDA Forest Service, PO Box 8089, Missoula MT 59807, USA (*author for correspondence, e-mail: deanu@pinus.env.duke.edu)

Received 10 December 1998; Revised 13 July 1999; Accepted: 9 October 1999

Key words: gap model, gradient analysis, landscape pattern, sensitivity analysis, Sierra Nevada, spatial scale, water balance

Abstract

Vegetation pattern on landscapes is the manifestation of physical gradients, biotic response to these gradients, and disturbances. Here we focus on the physical template as it governs the distribution of mixed-conifer forests in California's Sierra Nevada. We extended a forest simulation model to examine montane environmental gradients, emphasizing factors affecting the water balance in these summer-dry landscapes. The model simulates the soil moisture regime in terms of the interaction of water supply and demand: supply depends on precipitation and water storage, while evapotranspirational demand varies with solar radiation and temperature. The forest cover itself can affect the water balance via canopy interception and evapotranspiration. We simulated Sierran forests as slope facets, defined as gridded stands of homogeneous topographic exposure, and verified simulated gradient response against sample quadrats distributed across Sequoia National Park. We then performed a modified sensitivity analysis of abiotic factors governing the physical gradient. Importantly, the model's sensitivity to temperature, precipitation, and soil depth varies considerably over the physical template, particularly relative to elevation. The physical drivers of the water balance have characteristic spatial scales that differ by orders of magnitude. Across large spatial extents, temperature and precipitation as defined by elevation primarily govern the location of the mixed conifer zone. If the analysis is constrained to elevations within the mixed-conifer zone, local topography comes into play as it influences drainage. Soil depth varies considerably at all measured scales, and is especially dominant at fine (within-stand) scales. Physical site variables can influence soil moisture deficit either by affecting water supply or water demand; these effects have qualitatively different implications for forest response. These results have clear implications about purely inferential approaches to gradient analysis, and bear strongly on our ability to use correlative approaches in assessing the potential responses of montane forests to anthropogenic climatic change.

Introduction

There are three primary agents of pattern formation on terrestrial landscapes. *Abiotic constraints* such as elevation gradients, soil heterogeneity, and microclimate as effected by topography provide a physical template for ecosystem processes. *Biotic processes* such as demographic mechanisms (establishment, growth, and mortality), intra- and interspecific competition, and

dispersal generate a dynamic pattern on this template (Watt 1947, Smith and Huston 1989). Finally, *disturbance regimes* overlay onto this primary pattern, reacting to and interacting with the abiotic and biotic agents of pattern formation. Various authors have illustrated how these agents act and interact at various scales (Delcourt et al. 1983, Urban et al. 1987), yet it has proven remarkably difficult to isolate agents or to account their relative importance in real landscapes.

Table 1. Names and life-history parameters of tree species simulated for Sierran conifer forests.

Species	Common name	D_{\max}^1	H_{\max}^1	A_{\max}^2
<i>Abies concolor</i>	White fir	200	70	500
<i>Abies magnifica</i>	Red fir	200	70	500
<i>Calocedrus decurrens</i>	Incense-cedar	200	50	550
<i>Pinus contorta</i>	Lodgepole pine	100	50	300
<i>Pinus jeffreyi</i>	Jeffrey pine	200	60	700
<i>Pinus lambertiana</i>	Sugar pine	300	70	500
<i>Pinus monticola</i>	Western white pine	100	60	500
<i>Pinus ponderosa</i>	Ponderosa pine	300	65	700
<i>Quercus kelloggii</i>	Black Oak	100	30	300

Plant ecologists have a long tradition in the use of gradient analysis to infer the relative importance of environmental factors governing plant species distribution (see Stephenson 1990, for a review). Studies over the past few decades show a strong consensus on the relative importance of abiotic constraints in explaining gradients over hillslopes and mountainsides. Consistently, temperature and moisture emerge as the principal axes of direct and indirect gradient analyses. In the case of indirect gradient analysis, these factors are often inferred rather than measured directly: temperature is indexed as elevation or latitude, and soil moisture as an exposure index or drought scalar (Stephenson 1998).

Interpretation of gradient response is confounded by a fundamental lack of independence among environmental factors. In particular, the primary physical gradients of temperature and soil moisture are themselves correlated and thus not easily separable. For example, temperature decreases while precipitation increases with increasing elevation. Further, temperature is identified as a separate axis in gradient studies but it directly affects evaporative demand and so cannot be isolated from the soil moisture gradient. Thus, while it is easy to label an ordination axis 'temperature' or 'moisture' these labels do little to elucidate the underlying abiotic gradient complex.

Here we address the agents of pattern formation in forested landscapes, focusing on the physical template of forest pattern in montane landscapes of the southern Sierra Nevada in California, USA. In companion papers, we explore tree demographic response to this template (Urban, in prep.) and the disturbance (fire) regime (Miller and Urban 1999a–c). We use a spatially implemented forest simulation model to as-

Table 1 continued. Environmental response parameters of tree species simulated for Sierran conifer forests.

Species	Growth ³	Light ⁴	Drought ⁵	GDD ⁶
<i>Abies concolor</i>	1550	4	175	265
<i>Abies magnifica</i>	1050	4	140	50
<i>Calocedrus decurrens</i>	2150	3	185	555
<i>Pinus contorta</i>	2250	2	150	0
<i>Pinus jeffreyi</i>	1750	2	165	145
<i>Pinus lambertiana</i>	2450	3	165	430
<i>Pinus monticola</i>	1050	3	130	0
<i>Pinus ponderosa</i>	2350	2	185	750
<i>Quercus kelloggii</i>	1250	1	185	590

¹Maximum diameter (cm) and maximum height (m) were estimated from values observed for trees measured in adjacent National Forest lands (J. Verner, U.S.F.S., pers. comm. of unpublished Forest Service data).

²Maximum age estimates taken from Minore (1979) or Burns and Honkala (1990).

³Growth rate is nominally in units of $\text{cm}^3 \text{ wood m}^{-2} \text{ LAI}$, but is calibrated to field measurements.

⁴Shade tolerance class (1=very intolerant, 5=very tolerant) (Minore 1979, Burns and Honkala 1990).

⁵Drought tolerance, as maximum sustainable number of drought-days. These values are as calculated by the soil water component of the forest model FM, for sandy loams at a range of depths.

⁶Growing degree-days at the upper-elevation limit of the species distribution in the study area. This value is calibrated to reproduce observed species patterns, using degree-days as estimated within the forest model FM.

sess the relative importance of specific site variables as these contribute to temperature and soil moisture gradients in Sequoia National Park. We describe the characteristic spatial scaling of physical site variables (elevation, slope aspect, topographic convergence, and soil depth) as represented at the scale of a large basin, a small watershed, and a forest stand. Our analyses underscore the importance of the water balance in governing these summer-dry systems, but simulations also illustrate that simple interpretations of the observed patterns could lead to false inferences about underlying processes. Our findings have important implications for studies that use present-day gradient response as a basis for speculations about possible forest responses to anthropogenic climatic change.

Study area

Our study focuses on Sequoia National Park in the southern Sierra Nevada of California, USA (36°35' N, 118°35' W). The Park encompasses a striking physical gradient, spanning 4000 m relief over less than 100 km distance. Vegetation ranges from foothill grassland

and chaparral, through Ponderosa pine, the mixed conifer zone, red fir and lodgepole pine, to high-elevation western white pine near treeline (see species names in Table 1). Previous studies in the area have established a reasonable appreciation for the primary factors shaping forest pattern (Vankat 1982, Stephenson 1988, 1998). In particular, Stephenson's (1988, 1998) previous study of the soil water balance has tempered much of our work. In this mediterranean climate, roughly 95% of total annual precipitation falls from October through May, with monthly totals less than 1 cm typical of July and August.

Methods

Our modeling effort is part of a larger consortium of projects under the aegis of the National Park Service's (now Biological Resources Division of the US Geological Survey) Global Change Research initiative (Stephenson and Parsons 1993). Consistent with this initiative, an important objective was to position our group to make useful projections about how these systems might respond to climatic change. An equally important goal has been to provide a framework for integrating a variety of interrelated studies, both as the project was developed and, in the future, to incorporate new results from these ongoing studies. An explicit goal was to produce a model that could be used to extrapolate small-scale (stand-level) data to larger (landscape) spatial scales and long (centuries) time scales. This paper presents a benchmark in our efforts.

Botkin (1993) refers to several 'levels of assumptions' in model development. At a high level, the conceptual model is assumed to be an adequate representation of a system. At an intermediate level, the algorithms and formulations used in the model are assumed to adequately reproduce the processes of interest. At a lower level, the actual parameterization of these equations are assumed to fit the data adequately over the model's domain. Our goal has been to develop a model that is general and robust at the high and intermediate levels, while acknowledging that additional data could improve the parameterization of the model.

Model development

We extended a forest gap model (Urban et al. 1991, Urban and Shugart 1992) for the Sierra Nevada by expanding its physical routines (radiation, temperature, precipitation) in support of its new soil moisture

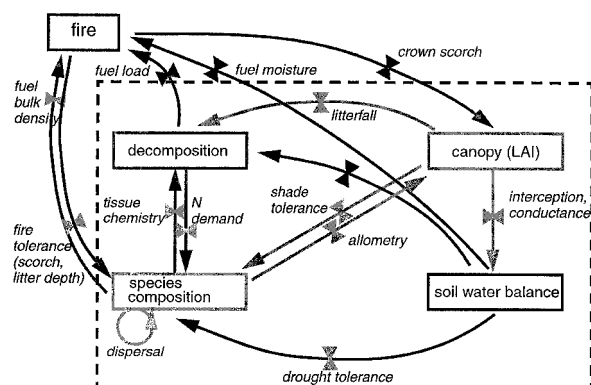


Figure 1. Schematic of feedback relationships in the main sub-models of Facet version FM 97.5. Arrows indicate significant interactions; those mediated by species-level differences are emphasized.

model, adding a new fire model, and parameterizing it for Sierran mixed-conifer forests. As a forest ecosystem model, the gap model couples several modules, only some of which are important for any given application (Figure 1). For the Sierra Nevada, soil moisture and fire are clearly dominant components of the system. The fire model, which couples forest dynamics, climate, and fire, is described elsewhere (Miller and Urban 1999a-c). Litter decomposition/nutrient cycling is tied to the fire model as the same data structures are used as decay classes and fuel types. The light regime is coupled to the water balance through interception and the influence of leaf area on transpirational demand. We have not invoked seed dispersal for this application because it is a distraction from our primary focus on temperature and soil moisture gradients. In this paper we focus on the soil water balance as it drives much of the rest of the model.

The model simulates a forest stand as a rectangular grid of 'tree-sized' cells (here, 15 × 15 m). Each grid cell corresponds to a conventional gap model plot, with the extension that trees may shade (or be shaded by) trees on nearby cells. The model assumes horizontal homogeneity at the scale of the cell, retaining the simplifying assumption that has helped make gap models so successful as a class of models (see Botkin et al. 1972, Botkin 1993, Shugart 1984). The model simulates a slope facet as the fundamental analysis unit in mountainous terrain (Daly et al. 1994). The modeled grid has a user-specified elevation, slope, and aspect. Climate parameters (minimum and maximum temperature; precipitation) are internally adjusted for elevation and topography using locally regressed lapse rates and radiation is predicted

and adjusted for topography (see below). Reflecting its topographically-adjusted implementation, we refer to this version as the FACET Model, or simply FM. Here we document the benchmark edition of the model, version FM 97.5.

The light regime

The crux of the light regime is a leaf area profile defined for each cell of the grid. This array is constructed by estimating total leaf area for each tree on the plot, and distributing this leaf area along each tree's live crown (after Leemans and Prentice 1987).

We predict tree height from diameter at breast height (1.37 m, dbh):

$$H = H_{\max} \left(1 - e^{h_1 D}\right)^{h_2}, \quad (1)$$

where D is dbh (cm), H_{\max} is maximum height (m), and h_1 and h_2 are fitted shape coefficients. Leaf area is predicted from sapwood cross-sectional area at the base of the tree's live crown (Waring et al. 1982, Waring and Schlesinger 1985). We use taper equations (Kozak et al. 1969) to predict diameter at base of crown, predict sapwood width from diameter (Lassen and Okkonen 1969), and estimate sapwood area by differencing off the heartwood; leaf area (m^2) is then predicted from a sapwood: leaf area ratio for that species. Leaf area is distributed uniformly over 1-m height intervals from treetop down to a species-specific light compensation point; foliage below this point is assumed to be lost permanently. Thus, trees of the same size and species may have different foliage profiles depending on the number and sizes of other trees shading them. The model aggregates the foliage profiles of each tree on each plot each simulation year.

The leaf area profile is used to estimate the light profile for each position (grid row, column, and height) within the modeled stand. FM does this by partitioning light into direct-beam and diffuse-sky components, and 'sampling' the forest canopy to estimate each component (Urban and Shugart 1992). This sampling is accomplished by constructing diagonal leaf area profiles by 'looking through' the vertical leaf-area array at a specified angle and direction. The direct-beam component is estimated by constructing a diagonal profile to the south, with a look angle derived from mean solar inclination angle as integrated over the growing season (Bonan 1989). The diffuse-sky component is estimated with multiple samples of the sky, by constructing diagonal profiles at various look angles and directions. Light impinging through

the diagonal leaf area profile is attenuated according to the Beer-Lambert Law:

$$S_h = S_0 e^{-k \Sigma L_h}, \quad (2)$$

where S_h is light at height h , S_0 is light at the top of the canopy, ΣL_h is leaf area index ($\text{m}^2 \text{m}^{-2}$) above height h , and k is an extinction coefficient here set to 0.4 (Jarvis and Leverenz 1983). Total light impinging at any point within the stand (row, column, height) is the sum of direct-beam and diffuse radiation.

FM predicts incident radiation S_0 for the grid by estimating net solar radiation for a horizontal surface and adjusting this for slope and aspect. In this, mean monthly net radiation (Ly day^{-1}) is predicted from latitude, topographic position, and cloudiness (Nikolov and Zeller 1992). Horizontal-surface radiation is adjusted for slope and aspect using geometric 'tilt factors' (Bonan 1989). Because the model grid is draped over the specified slope facet, the light regime is adjusted doubly for slope. First, a south-facing slope receives more incident radiation than a corresponding north-facing slope at this latitude. Secondly, because the grid cells are draped over a slope, on a steep north slope the path of light through the canopy is extremely long, while on a south slope the path from lower-canopy to open sky is comparatively short; light penetrates more deeply into the canopy on a south-facing slope.

The soil moisture regime

The soil water submodel simulates the soil water balance for a multi-layer soil. The gridded forest is underlain by a soils map which assigns a soil type to each cell. Each soil type is defined by the depth and water-holding capacity for each soil layer. Soil water dynamics are influenced by the canopy through interception and transpiration, and so even for the same soil type the soil water balance may vary uniquely for each grid cell in response to changing leaf area.

FM simulates soil moisture dynamics as the interaction of water demand and water supply. Demand is based on temperature and radiation, and so varies with elevation and topographic position. Water supply depends on water inputs and water storage. Inputs may be through precipitation or snowmelt, and storage is a function of soil depth and texture. Water-holding capacity of each soil layer is indexed by its content at field capacity (-0.01 MPa) and wilting point (-1.5 MPa). The uppermost layer in the soil profile is the litter layer, which changes dynamically through litterfall and decomposition and so the litter layer has

a water-holding capacity that varies dynamically as its depth varies.

The model works on a monthly timestep in that it uses monthly data for average minimum and maximum temperatures and total monthly precipitation. Precipitation events are simulated on a daily timestep (see below). Some processes are treated differently for months in the growing season as compared to the nongrowing season; the beginning and ending months of the growing season are estimated from a threshold minimum temperature. In terms of processing logic, the model predicts potential evapotranspiration (PET), and attempts to meet this demand via precipitation (including interception). If precipitation is less than PET, soil water storage is drawn down to meet water demand as long as soil water is available. After soil water is exhausted, unmet demand accrues as soil water deficit and actual evapotranspiration (AET) is less than PET. That is, climatic moisture deficit is PET minus AET.

FM uses a Priestley-Taylor estimate of potential evapotranspiration as implemented by Bonan (1989). PET is partitioned into two components. Active leaf area on a plot determines the proportion of PET expected as transpiration, estimated as:

$$E_t = 1 - e^{-kL}, \quad (3)$$

where L is leaf area index ($\text{m}^2 \text{m}^{-2}$) during the growing season, otherwise 0.0. Here, the coefficient k is set to 0.7 (Saugier and Katerji 1991). The model attempts to meet the remainder of PET ($1 - E_t$) via surface evaporation. Surface evaporation comes from the litter/duff layer first, with unmet demand drawn from the top mineral soil layer.

Transpiration, likewise, is drawn first from the top layers, but may also be drawn from deeper layers. In the algorithm, water is drawn off from the top layers downward, with unmet demand drawn from increasingly deeper layers in the soil as the soil dries. Likewise, soil water is recharged from the top down. In the summer-dry Sierra Nevada, this means that the soil dries down as the summer progresses, and is recharged in late fall when the rains resume.

Water inputs are from precipitation and snowmelt. The model uses a daily timestep to generate stochastic precipitation events, with event sizes and frequencies estimated from long-term data. Precipitation is partitioned into rain *versus* snow as a function of temperature (Aber and Federer 1992), using a function calibrated from local data. Snow is accumulated as water equivalents (cm) during the winter and then melted

in springtime using a simple melt rate specified in $\text{cm } ^\circ\text{C}^{-1} \text{ day}^{-1}$ (Running and Coughlan 1988).

During the growing season, interception is a function of leaf surface area on the plot, estimated by adjusting each grid cell's leaf area on a monthly basis. In the off season, deciduous species contribute an 'effective leaf area' to interception to represent woody surface area of branches and stems (Whittaker and Woodwell 1967); evergreen trees contribute intercepting leaf area year-round. The fraction of precipitation intercepted is a function of intercepting surface area:

$$I = 0.02L + 0.02LP, \quad (4)$$

where L is leaf area index and P is precipitation. Here, the first term is canopy storage and the latter term specifies an increasing proportion of total precipitation intercepted with increasing LAI. The estimate is set to 0.0 if $P = 0$ and to total precipitation if $I > P$. This approach is consistent with empirical summaries (Helvey and Patric 1965, Zinke 1967, Helvey 1971, Dingman 1994) but ensures that interception varies dynamically with canopy development. The model does not deal with the complexities of within-storm dynamics of interception such as those due to saturation of the leaf surface or within-storm evaporation. Water lost to interception is subtracted from PET.

The soil water balance is a modified 'tipping bucket' algorithm. Stochastic precipitation is generated, some is intercepted, and throughfall plus snowmelt comprise water input. First, a 'fast-flow fraction' of water input representing macropore flow flows through the soil and is lost as deep percolation. Next, the water input (rain plus snowmelt) is added to the top (litter) layer, and evaporative demand is removed if possible. Stored water is drawn down when water input is less than PET in any layer. A simple linear drawdown curve is invoked when soil water content is less than a critical water content (Sellers 1965). Unmet transpirational demand is carried to deeper soil layers, while evaporative demand is restricted to the litter and top soil layer. Water in excess of the bottom-layer field capacity, if any, is lost as deep percolation or subsurface flow. There is no lateral hydrologic flow between plots (grid cells) in this version of the model.

The model tallies two drought-day indices to summarize the soil water balance. A drought-day is a day during the growing season for which soil water is at or below wilting point. Drought-days are accrued on a daily basis throughout the growing season. The first index is integrated over the upper soil layers (top 20 cm)

to provide a topsoil moisture index. The second index is integrated over the fine-root density distribution in the entire profile to provide a whole-profile index. Following Bonan (1989), we model the distribution of fine roots as triangular with depth, a simple approach that places $\sim 80\%$ of fine roots in the upper 30 cm of a 1-m soil. The topsoil index is used to constrain seedling establishment, while the whole-profile index is used as a constraint on diameter growth rates of established trees.

The soil water routine is coupled indirectly to canopy development; trees do not actually 'transpire' water. Open canopies lead to dry-down of the uppermost layer due to increased surface evaporation. At the same time, stand thinning (including gap-creating mortality events) relieves the transpirational demand on the soil profile, and reduced transpiration may more than compensate for increased surface evaporation: topsoil moisture may show a net increase following the creation of a gap. The balance between wetting and drying in the topsoil (i.e., the top 20 cm) depends very much on the balance between surface evaporation (which increases in a gap) and subsurface transpiration (which decreases in a gap). This routine is thus simple yet quite responsive to canopy development.

Tree demographics

Although our emphasis here is on the physical template of forest pattern, the model couples physical routines to demographic processes and so we cannot avoid presenting these biotic routines here. Our intention here is to provide a conceptual overview, deferring a more detailed presentation to a subsequent companion paper.

The model simulates the processes of seedling establishment, annual diameter growth, and mortality for each tree on each cell of the simulated grid. These processes are simulated with a common logic of specifying the maximum potential a tree might achieve and then reducing this potential to reflect suboptimal environmental conditions. Simple scaling functions are used to describe these environmental responses (Figure 2; Urban and Shugart 1992).

Establishment. Seedling establishment is strongly keyed to light available at ground level and to the moisture status of the topsoil. Each species has a maximum possible establishment rate (seedlings $\text{plot}^{-1} \text{yr}^{-1}$). Each simulation year, species are 'filtered' (*sensu* Harper 1977) by the environmental response scaling functions that reduce the optimum rate.

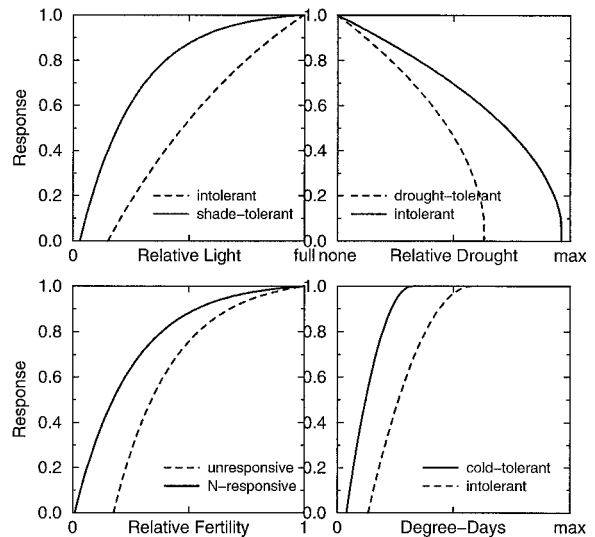


Figure 2. Species response functions used to scale seedling establishment rates and diameter growth in relation to (a) available light as proportion of full sun, (b) soil moisture deficit as drought-days, (c) relative soil fertility as N supply/demand, and (d) temperature as growing degree-days. Curves are examples of contrasting species tolerances; actual values vary by species (temperature, drought) or tolerance class (light, nutrients) (see Urban and Shugart 1992, for details).

Filtered seedlings are then 'planted' as a cohort of seedlings. These cohorts are tracked through a number of lag years defined as the minimum time it takes a species to reach 2.5 cm dbh, and then established as trees.

Growth. Tree growth is modeled deterministically via a function that describes the maximum potential diameter increment that could be achieved by a tree of a given species and size under optimal environmental conditions. The optimal growth increment is further reduced to reflect shading, soil-moisture deficit, low soil fertility (we simulate only nitrogen), or low temperature. The effect of shading is modeled by integrating the shade response function over a tree's canopy. Soil moisture affects tree growth by slowing growth as a species-specific maximum drought-day index is approached. Nutrient response is simulated in terms of N supply and demand for the plot. N supply is estimated as that N mineralized by the respiration of C in litter and woody debris, as implied by the C:N ratio of these tissues (after Parton et al. 1987, with some formulations taken directly from the CENTURY model). The N demand term is estimated allometrically for all trees on the plot, based on expected biomass increments and tissue chemistry for foliage, fine roots,

and wood for each species. The temperature response in this model is a departure from previous gap models, which have been much criticized for the way they model temperature effects on tree growth (Weinstein 1991, Bonan and Sirois 1992, Urban et al. 1993, Loehle and LeBlanc 1996). Here we assume that there exists a cold temperature at which species response is low for physiological reasons. Conversely, at this latitude the apparent response to high temperature is largely expressed through temperature's effect on the water balance – masking any direct effect on tree physiology. Thus, we use a one-sided response curve that reduces performance at low temperatures but is inoperative at high temperatures. This approach is consistent with studies of tree-rings in our study area, where trees at high elevations show stronger correlations with long-term variation in temperature, while tree-ring chronologies at low elevations are more correlated with variation in precipitation (L. Graumlich, Laboratory of Tree-Ring Research, University of Arizona, pers. comm.).

Environmental factors interact to constrain tree growth. We assume an interaction between above- and below-ground constraints, but assume that moisture and nutrients are so tightly interrelated as to be inseparable for our purposes. Thus, the overall constraint is the product of the temperature, light, and a below-ground factor, where the below-ground factor is the minimum of moisture or nutrients.

Mortality. Trees may die for three reasons in the model. There is a low ambient rate of purely stochastic mortality that is estimated from expected species longevity; this annual probability is age- and size-independent and for these species is on the order of ~1% per year. A second cause of mortality is lack of vigor, which is invoked when a tree fails to achieve 10% of its optimal growth for more than two successive years. Under these conditions a tree has an annual mortality probability corresponding to an expectation that it might survive 10 years under loss of vigor. Note that this approach, invoked similarly for all species, still results in very different mortality schedules for species that vary in their environmental tolerances. A third source of mortality is through fire, in which the probability of fire mortality is predicted from fireline intensity and tree characteristics (Miller and Urban 1999a).

Table 2. Lapse rates ($^{\circ}\text{C } 1000 \text{ m}^{-1}$) for monthly mean minimum and maximum daily temperature and mean monthly precipitation ($\text{cm } 1000 \text{ m}^{-1}$), as regressed¹ from seven meteorological stations² in Sequoia-Kings Canyon National Park.

Month	T_{\min}	T_{\max}	Ppt
January	5.71	5.40	3.93
February	6.49	5.39	5.08
March	6.66	6.75	4.48
April	6.51	7.29	1.33
May	6.42	8.06	0.78
June	6.84	7.98	0.21
July	6.88	7.68	0.42
August	6.67	7.76	0.19
September	6.90	7.99	1.12
October	6.42	7.32	1.16
November	5.52	6.39	3.06
December	5.34	5.68	4.11

¹Regression is $T = b_0 - b_1 E$, where E is elevation (m) and T is mean monthly temperature ($^{\circ}\text{C}$). All regressions are significant at $p < 0.0001$.

²Sites (with elevation, m) are: Visalia (100), Orange Cove (132), Lemon Cove (158), Ash Mountain (526), Giant Forest (1957), Grant Grove (2031), and Tyndall Creek (3298).

Model parameterization

Implementation of the model requires estimates for two primary sets of parameters, describing the physical site and the local tree species. Site parameters consist of climate and soils data, while species parameters include life-history traits, environmental responses, and demographic rates. A third, and optional, set of parameters for the fire submodel is required only if fires are invoked.

Site parameters. We used data from 7 meteorological stations in the Park to regress lapse rates for mean daily minimum and maximum temperature for each month and for total monthly precipitation (Table 2). For our sites, the precipitation lapse is truncated at an elevation of 2000 m, above which there is no further increase in precipitation. The fraction falling as snow is predicted from temperature, and snow is adjusted for gauge bias (Stephenson 1988).

Although the Park commissioned a detailed soils map for one region of our study area, we generally lack soils data of sufficient resolution to assign hydraulic parameters with confidence. Instead, we used the existing survey to develop a set of soils that reflect the range of soil types in the Park, and then

varied soil type and depth to simulate a wide variety of sites. For soils of different texture, we estimated water-holding capacity by regression on sand, silt, and clay fractions (Cosby et al. 1984). Most of the soils in the mid-elevation mixed-conifer zone are sandy loams of rather similar parent material and texture, and so we concentrated on depth as the primary variable in our simulations. At high elevations cryogenic soils are more typical, but as we have concentrated on the mixed-conifer zone we do not explore these other soil groups here.

Species parameters. We collated species information and data from a variety of local sources, expanding our search regionally when local sources were insufficient (Table 1). We used vegetation data collected by Stephenson (1988) and additional plot data collected as part of the Park's Natural Resource Inventory program (Graber et al. 1993). These samples are 0.1-ha quadrats distributed over much of the Park (randomly by Stephenson, $N = 228$; stratified by Graber et al., $N = 600$). As some of these quadrats located in nonforest vegetation were not used, our total pooled sample size was 584 quadrats. Each quadrat included tallies of each tree by species and diameter, as well as selected site data; slope, aspect, elevation, and surface rockiness are common to both data sets. Tree height allometries were estimated by regression, using height-diameter data collected in the adjacent National Forest by Forest Service personnel (J. Verner, USFS PSW Research Station, pers. comm. of unpublished data). Taper equations were computed from data maintained by the USDA Forest Service (S. Garman, Forest Sciences Lab, Corvallis, Oregon; unpublished data). Sapwood:leaf area ratios were generally unavailable for our species and so we used estimates from similar species (Waring et al. 1982, Waring and Schlesinger 1985). Similarly, we substituted parameters for common species when we lacked data for less common species (e.g., we used Ponderosa pine allometries for Jeffrey pine). Growth rates were estimated to fit tree ring data collected within the Park (D. Urban, unpublished data).

For some parameters the model is quite data-intensive (e.g., height-diameter allometries are based on more than 1000 trees for some species). In other cases we had a strong consensus in the literature as to rank differences among species (Minore 1979), but no specific quantitative information for parameter estimation (e.g., we knew relative drought tolerance but not actual drought-days for species). We performed an

initial calibration of the model using minimum degree-days, maximum drought-days, and species growth rate. We began by assigning drought tolerances corresponding to the drought-day indices simulated for sites at the lowest elevation where each species occurred (its driest site), and minimum degree-day limits corresponding to the maximum elevation for each species (its coolest site). We then freed these parameters in model calibration while forcing the estimates to remain consistent with accepted rank differences. Because species performance in a gap model depends on how each species performs relative to other species in the model, adjusting any species parameter also can alter the performance of all other species; and so model calibration is an iterative process that can quickly devolve into artless tinkering. Because we are still collecting demographic data to be used in a more rigorous model calibration, we have not pursued model calibration further at this point (see below).

Simulations

We performed two sorts of simulations. For *intensive* explorations of the model, we simulated single sites and scrutinized detailed output from the model. In these cases we also used a stand-alone version of the soil moisture model to provide month-by-month and soil layer-by-layer information on the water balance. For *extensive* explorations with the model, we simulated large numbers of cases in Monte Carlo fashion and analyzed summary statistics of model performance across a broad range of site conditions. In these latter, extensive explorations, we used a factorial design to stratify simulations across combinations of the primary site variables: elevation, slope, aspect, and soil type. We simulated 300 10×10 -cell model grids (2.25-ha stands) with elevation, slope, and aspect values drawn randomly from statistical distributions estimated from a digital elevation model for the Park (elevation and slope, gaussian; aspect, uniform). Soil depths were varied uniformly over values estimated from the soil survey and from field data (P. Halpin, unpublished data). Each simulation was for 50–250 yr, randomly distributed to provide a variety of successional ages (gaussian, mean age=150 yr). We used a distributed queuing system to perform the simulations (Urban et al., 1999).

Model verification

The radiation model performs quite well for a wide range of sites for which we have data. For a set of

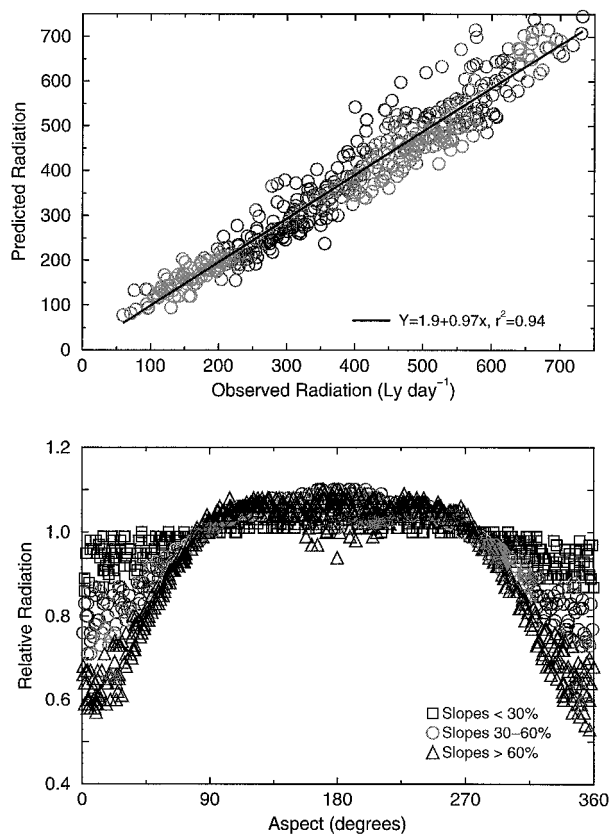


Figure 3. Solar radiation (direct + diffuse) as predicted with sub-program SOLAR in FM 97.5. (a) Verification of the model against data from 37 stations throughout North America (Mueller 1982). (b) Topographic patterns in radiation for a site at 2000 m in Sequoia National Park, relative to radiation for a horizontal surface.

37 stations across North America (Mueller 1982), the model reproduces monthly radiation values with an r^2 of 0.94 (Figure 3a). Because these are mostly primary meteorological stations (e.g., airports), we interpreted them as representing incident (above-canopy) radiation on horizontal surfaces and simulated them accordingly. Topographic exposure has a profound influence on radiation, with incident radiation levels relative to a horizontal surface varying with aspect for steeper slopes (Figure 3b).

We verified the soil water model qualitatively. Arkley (1981) and Anderson et al. (1995) measured soil moisture at various depths throughout a growing season at sites similar to mid-elevations in our study area. Their data show a substantial soil-moisture deficit that develops during the summer, with moisture contents near wilting point extending quite deeply (>2 m) into the soil profile and water potentials less than -2.0 MPa in the topsoil. These patterns are

Table 3. Distribution of tree species along elevation gradient in Sequoia National Park, from field data and as simulated using the FACET model. Standard deviation in parentheses. Asterisks indicates a significant difference according to permutation tests.¹

Species	Basal Area		Mean Elevation ⁴	
	Data ²	Model ³	Data	Model
<i>Abies concolor</i>	14.43 (21.89)	12.45 (18.33)	2047 (196)	2259** (216)
<i>Abies magnifica</i>	11.02 (25.78)	9.70 (17.71)	2574 (225)	2732** (169)
<i>Calocedrus decurrens</i>	2.23 (5.94)	2.92 (6.86)	1826 (218)	1864 (215)
<i>Pinus contorta</i>	2.92 (10.02)	6.03** (13.25)	2675 (141)	299** (234)
<i>Pinus jeffreyi</i>	1.28 (4.56)	1.99* (4.85)	2137 (177)	2185 (327)
<i>Pinus lambertiana</i>	3.10 (8.18)	2.99 (7.94)	2019 (157)	2201** (147)
<i>Pinus monticola</i>	1.00 (4.91)	1.97* (4.92)	2816 (189)	2975** (216)
<i>Pinus ponderosa</i>	1.83 (6.81)	3.87 (10.27)	1749 (190)	1838** (162)
<i>Quercus kelloggii</i>	0.93 (3.11)	0.30 (1.03)	1694 (227)	1685 (320)

¹Significance as 2-tailed test on 1000 random permutations of the plot labels ('data' or 'model'; see text). * $p < 0.05$; ** $p < 0.01$.

²Estimated from 280 0.1-ha sample plots from Kaweah Basin in Sequoia National Park (Stephenson 1988, Graber et al. 1993).

³Estimated from 300 simulated stands stratified across elevation, slope, aspect, and soil depth as represented in Kaweah Basin, at ages ranging from 50–250 yr.

⁴Mean elevation is weighted by relative basal area per sample (see text).

reproduced by our simulations. Ziemer (1964) also described patterns in soil moisture at depth in Sierran mixed conifer forests, emphasizing trends in soil moisture under clear-cuts as compared to intact forests. His figures show a relation between soil moisture draw-down and forest regrowth that is consistent with the relationship between transpiration and LAI simulated in the model.

Tree species distributions were verified using plot-level summary data derived from 280 sample quadrats distributed within the Kaweah Basin, a $\sim 90,000$ -ha basin that comprises the west slope Sequoia National Park. We limited the data geographically because rain shadow effects east of the Great Western Divide generate a moisture regime that is not well represented by available climate data. We summarized basal area

($\text{m}^2 \text{ha}^{-1}$) for 9 common species for the field data and the simulated plots (Table 3). We computed the difference in these mean scores, then permuted the labels on the plots (either ‘data’ or ‘model’) and tested the hypothesis that the labelling didn’t matter – that is, that the modeled and field plots were indistinguishable. Lodgepole pine, western white pine, and Ponderosa pine are somewhat overpredicted by the model while black oak is somewhat underpredicted. To test simulated species response to elevation, we compared the model-generated forests to field data by computing the abundance-weighted mean elevation for species j , E_j :

$$E_j = \sum_{i=1}^n \frac{b_{ji} \cdot e_i}{\Sigma b_j} \quad (5)$$

where b_{ji} is basal area ($\text{m}^2 \text{ha}^{-1}$) for species j on plot i , Σb_j is total basal area for species j over all n plots, and e_i is elevation of plot i . In fact, the model does not perform very well under this test: most species showed a significantly different mean elevation between model and data (Table 3). Despite this, the model does seem to capture the gross pattern of species response to the elevation gradient (Figure 4). We are reluctant to interpret discrepancies between modeled and empirical species abundances for two reasons. First, we lack information on the detailed site conditions (especially soil depth), stand age, and site history of the field samples. More importantly, we are still collecting demographic data that will be used to better calibrate the model. For our purpose of exploring the physical template, it is sufficient (indeed, necessary) that the model simulates canopies appropriate for the soil water model as it uses these to model interception and evapotranspiration. Similarly, the model generates fuel loads and litter accumulation rates consistent with measured values and appropriate for the fire model (Miller and Urban 1999a). Thus, we are content to note that with minimal calibration of the model using local field data, the simulator provides an adequate representation of these forests across a wide range of site conditions, but the details of species distributions can still be improved.

Model sensitivity analysis

In formal model sensitivity analysis (e.g., Gardner and Trabalka 1985, Haefner 1996) one systematically varies all model parameters by 10% of their nominal or mean values, and then regresses a selected output variable against the input variables in a multiple regression format. A parameter’s sensitivity is its regression

slope, i.e., the amount of change in the output variable associated with a small change in the input variable. In our case, this approach is not very satisfying for two reasons. First, temperature and precipitation both covary with elevation and so are collinear over most of their distributions; this renders the multiple regression somewhat pathological because either variable, once entered into the regression, masks the effect of the other variable. More importantly, the conventional sensitivity analysis does not clearly resolve instances where the sensitivity of a variable varies considerably over its domain. In this case, we expect the model’s sensitivity to temperature or precipitation to vary with elevation.

To assess the sensitivity of the model to its physical drivers, we generated 1500 combinations of elevation, slope, aspect, and soil depth and simulated these cases using the stand-alone version of the soil water model. We then simulated each of these cases again, manually adjusting temperature, precipitation, and soil depth by 10% of the baseline values. This resulted in 3 new sets of 3000 runs each, a total of 10,500 simulations including the baseline cases. We indexed model sensitivity to each input variable by differencing the drought-day index for the +10% as compared to the –10% case, yielding an index of δ (drought-days).

Spatial scaling of the physical template

We characterized the spatial scale of the physical template over three spatial extents. At the largest extent, we sampled terrain-based variables in a geographic information system (GIS) of the Kaweah Basin ($\sim 90,000$ ha), using a 30-m resolution DEM. From the DEM, we extracted elevation and aspect. We then transformed aspect (Beers et al. 1966):

$$A' = \cos(45 - A) + 1, \quad (6)$$

where A is aspect in degrees. This transformation takes on maximum and minimum values along a northeast-southwest axis. We also computed a topographic convergence index (TCI) based on terrain:

$$\text{TCI} = \ln \left(\frac{a}{\tan \beta} \right), \quad (7)$$

where a is upslope contributing area and β is local slope angle (Moore et al. 1990, Wolock and McCabe 1995). The index takes on high values in coves and other convergence zones, and low values on excessively drained ridges or outcrops. We sampled the DEM using random clusters of 3 points within a 100-m cluster radius. Excluding points that fell within the

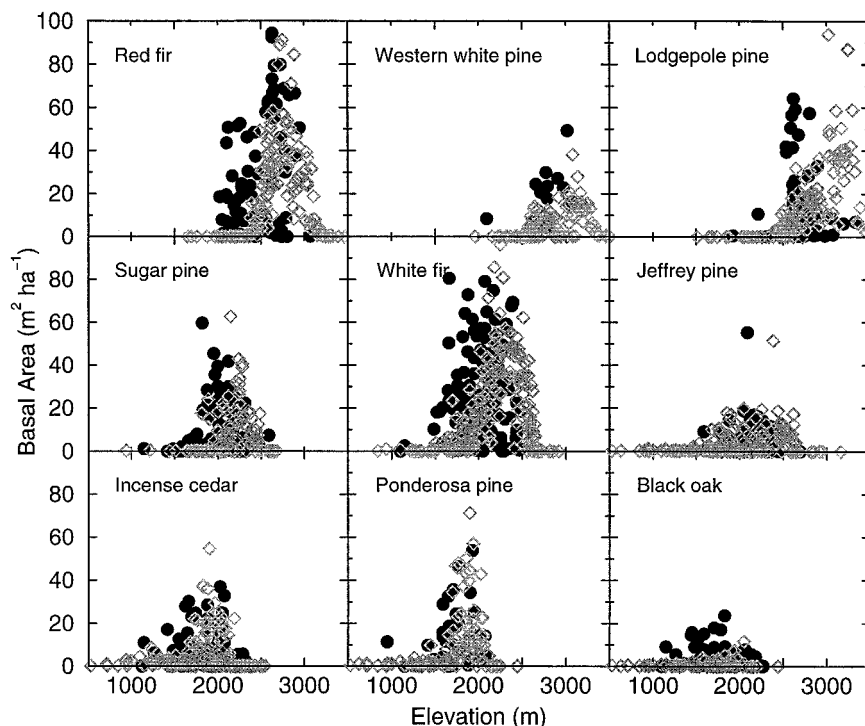


Figure 4. Species response to the elevation gradient in Kaweah Basin in Sequoia National Park, from 280 0.01-ha sample quadrats (filled circles) and as simulated for 300 slope facets defined by elevation, slope, aspect, and soil depth (open diamonds).

same 30-m cell or outside the basin boundaries, this yielded 20,903 samples ($\sim 0.015\%$ of the area) for geostatistical analysis of these terrain-based variables. We have no useful soils data over this large extent.

Over a smaller spatial extent, we analyzed Log Creek Watershed, a 50-ha watershed within the Kaweah Basin. The entire watershed was surveyed to create a digital elevation model with 5-m horizontal resolution (cell size). We collected the terrain-based variables by extracting elevation and its derived aspect and TCI values for every cell in the GIS grid, yielding 1075 points. Our scaling analysis for soil depth in Log Creek watershed was based on actual field measurements, which Halpin (1995) collected at 60-m intervals throughout the watershed ($N = 154$). Soil depth was measured with an auger to a maximum depth of 4 m.

Over a still smaller extent, we analyzed a 2.5-ha mixed-conifer reference stand within Log Creek Watershed. The stand was surveyed to create a DEM with 50-cm horizontal resolution. We extracted the DEM, aspect, and TCI from GIS coverages to yield 1750 sample points. For soil depth, Halpin sampled a 1-ha

section of this stand at 5-m intervals, yielding 100 field measurements of soil depth.

These data thus provide measures of the physical variables affecting the water balance at three spatial scales ranging over orders of magnitude in extent and with corresponding changes in grain (resolution). We use elevation as a proxy for temperature and precipitation. Transformed aspect is a proxy for radiation load, as it scales aspect relative to maximum afternoon sun. We included TCI because of its recognized relationship with soil moisture as governed by local drainage (Yeakley et al. 1998) even though our model, as a point model, does not simulate lateral hydrologic flow. Soil depth is a primary variable affecting water storage in this system. Thus, we analyzed the scaling of two demand terms (temperature and radiation) and three supply terms (precipitation, drainage, and storage). We assessed the characteristic scaling of these variables by computing semivariograms (Legendre and Fortin 1989). In each case, the distance interval (lag) was set to a value twice the spatial grain (cell size) of the measured variable and total distances were extended to half the minimum dimension of the study area.

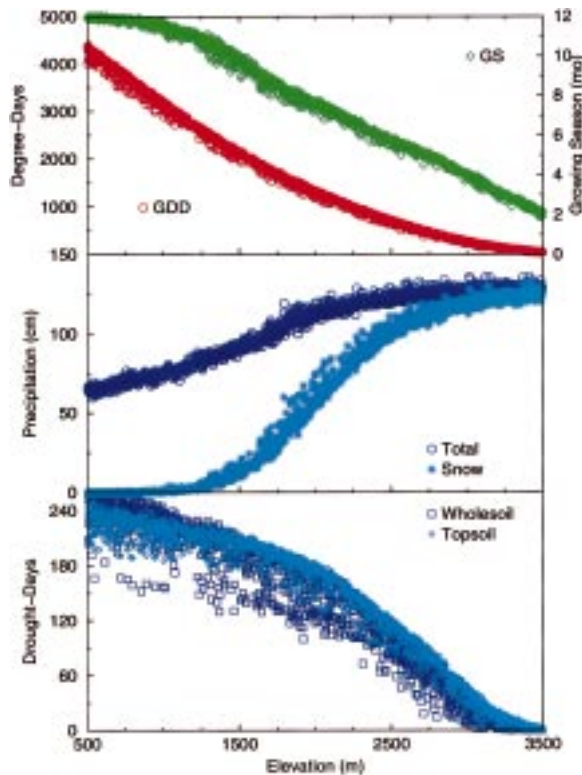


Figure 5. The physical template in Sequoia National Park. (a) Growing degree-days and duration of growing season. (b) Total annual precipitation and snow fraction. (c) Drought-day indices for topsoil and entire soil profile. Each point is a 100-year average for a site defined by its elevation, slope, aspect, and soil depth ($N = 1500$).

Results

We present simulation results by first characterizing the physical template of the study area in terms of the components of the water balance. We then examine these components in terms of their local sensitivity in the model and their characteristic spatial scaling.

The physical template as environmental gradient

Elevation dictates much of the pattern in the physical template as represented in Sierran landscapes. As elevation increases, monthly temperatures decrease linearly while the integrated growing-season heat sum (degree-days) decreases in a moderately nonlinear fashion (Figure 5a). At low elevations the growing season is essentially year-round insofar as temperature is concerned; by contrast, cold temperatures severely limit the growing season at the highest elevations that support trees in this area.

Precipitation increases linearly with elevation up to an elevation of 2000 m, above which it remains nearly constant. But because of the correction for gauge bias applied to the snow fraction, total precipitation continues to increase slightly above 2000 m (Figure 5b). More importantly, precipitation switches from predominantly rain at low elevations to snow at high elevations, with the split being roughly equal at the mid-elevations.

These physical variables interact to generate a soil moisture balance that varies in a nonlinear fashion with increasing elevation (Figure 5c). At low elevations precipitation falls as rain and is lost as deep percolation or runoff once the soil is saturated. High evaporative demand during the growing season prevents recharge of the deeper soil layers, and the vegetation grades from woodland to grassland where soil moisture is inadequate to sustain trees (seen as a lower drought-day index for the topsoil as compared to the entire soil profile at the lowest elevations in Figure 5c; at all other elevations the whole-soil drought index is lower than that of the topsoil). At mid-elevations the precipitation shifts to snow, and where the snowpack persists long enough to provide meltwater into the summer, the drought-day index decreases steeply. At high elevations, soil moisture is adequate for most of the year because cold temperatures provide such low evaporative demand that soil water is not exhausted; higher precipitation at these elevations is effectively moot, given the low temperatures. (We should note, however, that extremely shallow or rocky soils can exhibit droughtiness even at these high elevations.)

Model sensitivity

The model shows quite marked local sensitivity to slight variation in the driving variables, and as expected these sensitivities vary across the elevation gradient. The model's sensitivity to temperature is strongly nonlinear with a maximum sensitivity at elevations near 2700 m, above the upper ecotone of the mixed-conifer zone (Figure 6a). The model shows a similar sensitivity to precipitation at these elevations, but also exhibits a second zone of high local sensitivity at low elevations (Figure 6b). It should be noted that because of the temperature effect on the proportion of rain *versus* snow, the sensitivity at higher elevations reflects a change in the snowpack, while the lower-elevation sensitivity is to rain.

Sensitivity to soil depth varies with elevation as well as with soil depth itself (Figure 6c). In the former

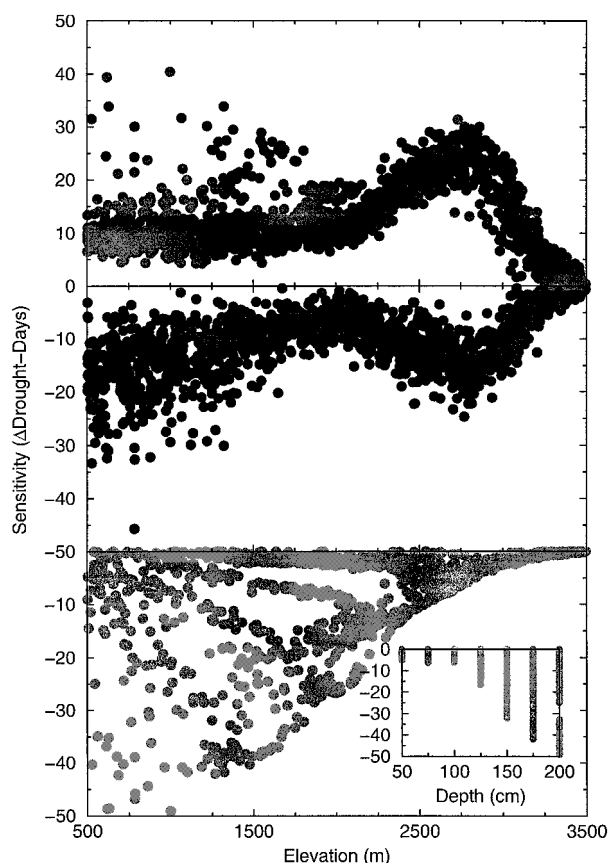


Figure 6. Local sensitivity of the soil water model to 10% variation in (a) temperature relative to elevation (b) precipitation relative to elevation, and (c) soil depth relative to elevation and (c) soil depth.

case, this reflects the relationship between evaporative demand and elevation as driven by temperature; high-elevation soils are largely insensitive to soil depth because water is rarely limiting. In the latter case, the effect is due to a threshold-like behavior in the soil water balance. Shallow soils that cannot meet growing-season evaporative demand are insensitive to slight variation in soil depth – they remain too shallow. By contrast, soils that are sufficiently deep to meet higher demand do respond to variation in depth. The depth at which this threshold occurs must vary with elevation because demand itself varies with elevation.

The sensitivity of the physical variables can be compared crudely in terms of the magnitude of change in drought-days they elicit in the analysis (the sign of this difference is arbitrary), which shows that the water balance can be quite responsive to any of these variables (they have similar maximum δ 's, as much as ~ 40 drought-days). Overall, temperature shows a slightly higher mean sensitivity (~ 13 drought-days) than pre-

cipitation (~ 7 drought-days) or soil depth (~ 11). But this average assessment detracts from the more important result that these variables are most responsive in particular locations.

Scaling of the physical template

The features of interest in a variogram are its sill (asymptotic value), range (the distance at which the sill is reached), and nugget (Y -intercept, reflecting variation finer-scale than the minimum lag distance). We present variograms with semivariance normalized by simple variance, so that the expected value for the sill is 1.0. Elevation exhibits the signature variogram of a simple gradient, with semivariance increasing monotonically at increasing lag distances (Figure 7). That is, there is no obvious grain to elevation within the scope of our study area. This is true at all three scales. Directional variograms (not shown) are similarly linear but with different slopes in different directions, reflecting the anisotropy in elevation in the study area as dictated by the N-S trending mountain range (Halpin 1995).

Other terrain-based variables are comparatively finer-scaled than elevation. At the basin scale, aspect approaches its sill value at a range of 800–1000 m, while TCI has a slightly smaller range on the order of 200 m (Figure 7a). Within the small watershed, both variables approach their sills at ranges of ~ 100 m, and soil depth shows a scaling similar to slope aspect (Figure 7b).

Within the spatially restricted domain of the forest stand, both aspect and TCI show large nugget variances indicating substantial variation at scales finer than the resolution of the analysis (Figure 7c). TCI appears to reach a sill at a range of 10–20 m, reflecting microtopography. Aspect does not reach a sill within this stand. Soil depth shows a variogram with a very large nugget variance and no obvious sill.

Presenting the variograms normalized by simple variance allows us to overlay the graphs for comparison but masks the change in total variance encountered as a function of scale. In fact, one would expect to encounter a range of variation at the basin, watershed, and stand scale that would reflect the spatial patterning of each variable. This expectation is met for elevation, which shows a dramatic decrease in its standard deviation as estimated at the basin, watershed, and stand scales (Table 4). By contrast, this trend does not hold for aspect, TCI, nor soil depth. Rather, for each of these variables, higher-resolution measure-

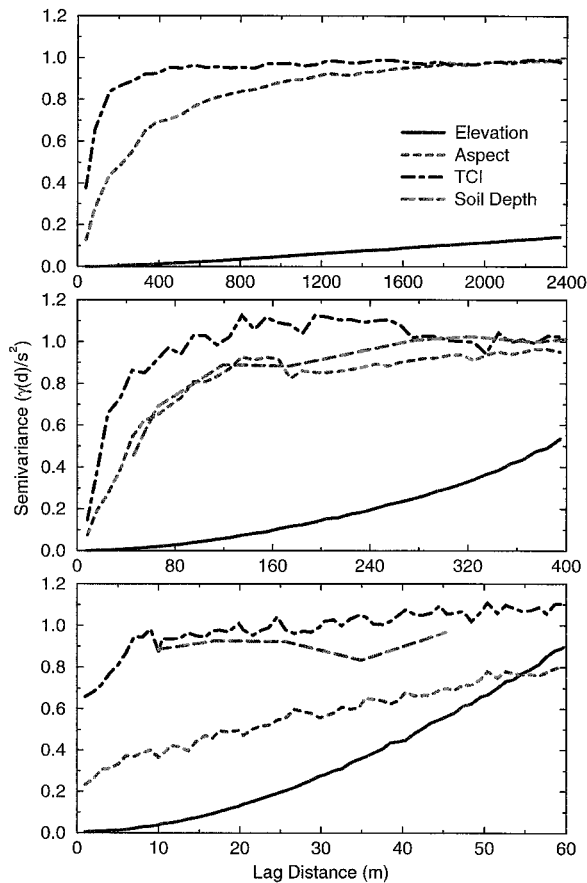


Figure 7. Spatial scaling, as semivariograms for elevation, aspect (transformed to a NE–SW axis), topographic convergence, and soil depth at three scales. (a) The 90,000-ha Kaweah Basin in Sequoia National Park. Data were sampled from 30-m resolution digital elevation model ($N = 20,903$) (no soil depth data available). (b) The 50-ha Log Creek Watershed in the Kaweah Basin. Terrain data were sampled from 5-m resolution digital elevation model ($N = 1075$). Soil depth was measured on 60-m interval throughout the watershed ($N = 154$). (c) A 2.5-ha mixed conifer stand in Log Creek Watershed. Terrain data were sampled from a 50-cm resolution digital elevation model ($N = 1750$). Soil depth was measured at 5-m intervals for a 1-ha central subsection of the stand ($N = 100$).

ments merely yield finer-scale expressions of the same variables.

Discussion

The nature of the physical template

The inflection of the drought-day curve (Figure 5c) corresponds roughly to the position of the mixed conifer zone in the study area (~ 1500 – 2500 m elevation). Thus, to a crude approximation we can envision

Table 4. Range of variability in elevation, aspect, topographic convergence (TCI), and soil depth as estimated at the basin, watershed, and stand scales. Tabled values are means (standard deviation) and sample sizes.

Scale	Elevation	Aspect ¹	TCI ²	Soil depth ³
Kaweah basin (90,000 ha; 30-m resolution)	2192.6 m (699.7)	0.784 (0.683)	6.31 (1.82)	no data
Log Creek watershed (50 ha; 5-m)	2245.5 (70.4)	0.472 (0.457)	7.82 (1.49)	168.4 cm (84.4)
Mixed conifer stand (2.5 ha; 50-cm)	2173.9 (8.6)	0.602 (0.628)	8.60 (1.89)	154 (50.7)
	$N = 20,093$	20,903	20,903	
	$N = 1075$	1075	1075	154
	$N = 1750$	1750	1750	100

¹ Aspect as transformed assumes values on $[0,2]$, 0=SW, 2=NE, SE=NW.

² TCI is a dimensionless, log-transformed ratio of area and slope, typically taking values on a range from near 0 (divergent ridges) to ~ 14 (deep coves).

³ Soil depth estimated from field measurements at the watershed and stand scale only.

the mixed-conifer zone as being compressed between a low-elevation constraint of droughtiness and a high-elevation boundary defined by cold temperatures.

Stephenson (1990, 1998) found it useful to consider the interactions of water supply *versus* demand as they effect vegetation distribution. He suggested that temperature and ‘moisture’ (indexed as topographic moisture scalars) should be abandoned as the primary axes of species response in vegetation studies. He argued that actual evapotranspiration (AET) and climatic moisture deficit (PET–AET) would be more relevant to plant response, and he illustrated the utility of this framework across scales from montane to continental gradients. This framework is especially useful for our purposes because it allows us to isolate specific factors of the physical template as these effect the water balance.

Our scaling analyses imply that the physical factors governing water supply operate at three different spatial scales corresponding to precipitation, drainage, and soil depth. By contrast, factors governing water demand (temperature, radiation) vary at two scales (elevation and microtopography). The characteristic scaling of the physical template is such that soil depth is the factor that is most variable over small spatial extents. At larger extents, variation in microtopography (slope, aspect, convergence) plays a more pronounced role in governing the water balance (al-

though soil depth continues to vary at these scales). At the scale of the Sierran range, variation in temperature and precipitation as governed by elevation and orography come into play as the primary constraints on the system. Note, however, at this largest scale that fine-scale variability cannot be resolved logistically. Conversely, at small scales temperature and precipitation are essentially constant and hence contribute little to an explanation of vegetation at these scales. Thus, explanations of forest pattern must be scale-specific and must invoke different proximate explanatory variables at different scales (an empirical demonstration of a general 'scaling principle' suggested by Wiens 1989). Importantly, the phenomenon being explained also varies with scale: temperature and precipitation provide a suitable explanation for the location of the mixed conifer zone but offer little to resolve the local distributions of tree species within this zone. Likewise, soils and microtopography help explain species distributions locally but these explanations cannot be extrapolated easily across larger, landscape-scale gradients.

Stephenson (1990, 1998) also suggested that acknowledging the different effects of supply *versus* demand components of the water balance was important because tree species respond differentially to these components. In fact, he argued that supply and demand represented nearly orthogonal vectors of response. For example, at middle elevations in the Kaweah Basin sites on deep soils support white fir forest; sites that are droughty because of shallow soils (low water supply) support Jeffrey pine, while sites that are droughty due to southerly aspect (high evaporative demand) instead support ponderosa pine (Figures 5 and 6 in Stephenson 1998). Although our model uses different estimates of supply and demand (*e.g.*, a Priestley Taylor PET as compared to Stephenson's earlier use of the Thornthwaite estimate), it reproduces the same qualitative result. To illustrate this, we graphed the water balance as an elevation gradient in a space defined by AET and water deficit. A change in water supply was simulated as a change in water storage, for a 50-cm *versus* a 150-cm soil. Change in water demand was illustrated with a change from northern to southern aspect for a 33% slope. These two vectors are indeed nearly orthogonal (Figure 8). Again, this implies that changes in the water balance mediated by changes in water demand as compared to water supply could elicit qualitatively different responses in the vegetation.

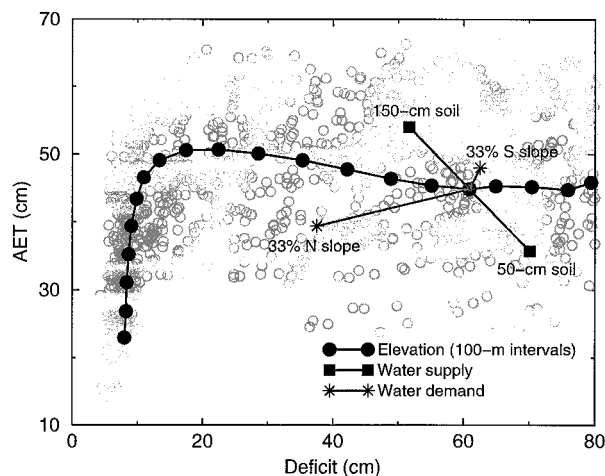


Figure 8. Components of the water balance simulated for Kaweah Basin in Sequoia National Park, as orthogonal vectors influencing water supply (as soil depth) as compared to water demand (as slope aspect). Baseline curve represents an elevation gradient at 100-m intervals, for a 1-m sandy loam on a horizontal surface. Supply and demand vectors are relative to this baseline at 2000 m. Pale circles are the range of variability expressed within the Kaweah Basin, illustrated with the 1500 cases simulated for Figure 5.

Implications under climatic change

This framework has important implications concerning anthropogenic climatic change. Many studies that have considered possible forest responses to greenhouse scenarios have assumed that the environmental responses of species can be inferred from observed distributions (*e.g.*, Solomon 1986, Urban et al. 1993; see Shugart et al. 1992, Smith et al. 1992, Loehle and LeBlanc 1996, for reviews). Even if this assumption were true, our results cast serious doubt on the utility of projecting these inferences to future-climate scenarios. These issues relate to the spatiotemporal scaling and interactions of the physical variables affecting species distributions.

First, while temperature and precipitation might well change under greenhouse scenarios, other factors affecting the water balance (terrain, soil depth and texture) will not. Further, there is no reason to believe that temperature and precipitation might continue to vary as they do in the current climate. Indeed, although current general circulation models (GCM's) all predict warmer temperatures for the study area under enhanced CO₂ scenarios (VEMAP 1995), the models do not agree on the direction of change in precipitation. While a crude space-for-time substitution would suggest that greenhouse scenarios would displace the mixed conifer zone upward perhaps hundreds of me-

ters, this approximation ignores the interaction of supply and demand components of the water balance as represented in the elevation gradient. The mixed conifer zone is defined by both temperature and precipitation as these interact through lapse rates affecting supply (precipitation) and demand (temperature), the partitioning of snow *versus* rain, the duration of snowpack, and the length of the growing season; all of these patterns are overlaid on the template of terrain and soils. Space-for-time substitution cannot embrace the complexities of these interactions.

The scaling of the physical template also suggests serious caveats when projecting the implications of anthropogenic climatic change. While it is true that temperature and precipitation can predict the location of the mixed conifer zone, it also is true that within this zone several species can co-occur over distances of tens to hundreds of meters, as defined by the spatial scaling of microtopography and soils. This high degree of spatial heterogeneity within the mixed conifer zone suggests that under climatic change, species might move around within that zone – more mesic species being displaced to deeper soils or more northerly exposures, more xeric species to shallower soils or more southerly exposures, with species abundances changing accordingly. Such comparatively fine-scale adjustments would be mediated by the ability of different species to disperse locally, a process mediated by seed dispersal distances measured on the order of tens of meters (Clark et al. 1999) – the same scale as variation in soils and microtopography, and much finer-scale than climatic variability.

A model that incorporates the effective components of the water balance can provide a robust framework and appreciation for the way in which these components interact to generate the spatiotemporal pattern of the physical template of montane systems. This framework attends the effective components of the environmental gradient complex and recognizes these at their characteristic spatiotemporal scales. The model is thus capable of integrating these processes and constraints to their coarse-scale definition of the mixed conifer zone as well as the finer-scale patterns associated with species distributions within this zone. We believe community and landscape ecology would benefit from a richer appreciation for the components of environmental gradient complexes and the way they interact to generate the physical template upon which all terrestrial processes play out.

Acknowledgements

This work was supported largely through USGS Biological Resources Division contract CA8800-1-9004 with additional support from NSF grants IBN-9652656 and DBI-9630606 to D. Urban. We appreciate the input from nearly two dozen collaborators in the Sierra Nevada Global Change Research Program. In particular, we would like to thank Annie Esperanza for her brokerage of the Park's data archives and Dave Graber for providing access to the Natural Resource Inventory data. Chi-ru Chang, Ken Pierce, and three anonymous reviewers provided constructive criticisms on an earlier draft of this manuscript.

References

- Aber, J.D and Federer, C.A. 1992. A generalized, lumped-parameter model of photosynthesis, evapotranspiration, and net primary production in temperate and boreal forest ecosystems. *Oecologia* 92: 463–474.
- Anderson, M.A., Graham, R.C., Alyanakian, G.J. and Martynn, D.Z. 1995. Late summer water status of soils and weathered bedrock in a Giant Sequoia grove. *Soil Science* 160: 415–422.
- Arkley, R.J., 1981. Soil moisture use by mixed conifer forest in a summer-dry climate. *Soil Sci Soc Am J* 45: 423–427.
- Beers, T.W. Press, P.E. and Wensel, L.C. 1966. Aspect transformation in site productivity research. *J For* 64: 691–692.
- Bonan, G.B. 1989. A computer model of the solar radiation, soil moisture, and soil thermal regimes in boreal forests. *Ecol Modelling* 45: 275–306.
- Bonan, G.B., and Sirois, L. 1992. Air temperature, tree growth, and the northern and southern range limits to *Picea mariana*. *J Veg Sci* 3: 495–506.
- Botkin, D.B. 1993. *Forest Dynamics: an Ecological Model*. Oxford University Press, Oxford.
- Botkin, D.B., Janak, J.F. and Wallis, J.R. 1972. Some ecological consequences of a computer model of forest growth. *J Ecol* 60: 849–873.
- Burns, R.M. and Honkala, B.H. (tech. coords.) 1990. *Silvics of North America. Agric Handbook 654*, USDA Forest Service, Washington, DC.
- Clark, J., Silman, M., Kern, R., Macklin, E. and HilleRisLambers, J. 1999. Generalized seed dispersal near and far: patterns across temperate and tropical forests. *Ecology* 80: 1475–1494.
- Cosby, B.J., Hornberger, G.M., Clapp R.B. and Ginn, T.R. 1984. A statistical analysis of the relationship of soil moisture characteristics to the physical properties of soils. *Wat Res Res* 20: 682–690.
- Daly, C., Neilson, R.P. and Phillips, D.L. 1994. A digital topographic model for distributing precipitation over mountainous terrain. *J Appl Meteor* 33: 140–158.
- Delcourt, H.R., Delcourt, P.A. and Webb, T. 1983. Dynamic plant ecology: the spectrum of vegetation change in space and time. *Quat Sci Rev* 1: 153–175.
- Dingman, S.L. 1994. *Physical Hydrology*. Macmillan, New York.
- Gardner, R.H., and Trabalka, J.R. 1985. *Methods of uncertainty analysis for a global carbon dioxide model*. Office of Energy Research, U.S. DOE, Washington, DC.

- Graber, D.M., Haultain, S.A. and Fessenden, J.E. 1993. Conducting a biological survey: a case study from Sequoia and Kings Canyon National Parks. pp. 17–35. *In* Proceedings of the Fourth Conference on Research in California's National Parks. Edited by Veirs, S.D. Jr., Stohlgren, T.J. and Schonewald-Cox, C. U.S. Department of the Interior National Park Service Transactions and Proceedings Series 9.
- Haefner, J.W. 1996. Modeling biological systems: principle and applications. Chapman and Hall, New York.
- Halpin, P.N. 1995. A cross-scale analysis of environmental gradients and forest pattern in the giant sequoia-mixed conifer forest of the Sierra Nevada. Ph.D. dissertation. University of Virginia, Charlottesville.
- Harper, J.L. 1977. Population biology of plants. Academic Press, New York.
- Helvey J.D. 1971. A summary of rainfall interception by certain conifers of North America. Pp. 103–113. *In* Proc. Third International. Symp. for Hydrology Professors, Biological Effects in the Hydrologic Cycle. Purdue Univ Agric Expt Station, West Lafayette.
- Helvey, J.D. and Patric, J.H. 1965. Canopy and litter interception of rainfall by hardwoods of eastern United States. *Water Res Res* 1: 193–206.
- Jarvis, P.G. and Leverenz, J.W. 1983. Productivity of temperate evergreen and deciduous forests. pp. 234–261. *In* Physiological Plant Ecology, vol. IV. Edited by Lange, O.L., Nobel, P.S., Osmond, C.B. and Ziegler, H. Springer-Verlag, Berlin
- Kozak, A., Munro, D.D. and Smith, J.H.G. Taper equations and their application in forest inventory. *For Chron* 45: 278–283.
- Lassen, L.E. and Okkonen, E.A. 1969. Sapwood thickness of Douglas-fir and five other western softwoods. USDA For Serv Rep FPL-124. Forest Products Lab, Madison, WI.
- Leemans, R. and Prentice, I.C. 1987. Description and simulation of tree-layer composition and size distribution in a primaeval *Picea-Pinus* forest. *Vegetatio* 69: 147–156.
- Legendre, P. and Fortin, M.J. 1989. Spatial pattern and ecological analysis. *Vegetatio* 80: 107–138.
- Loehle, C. and LeBlanc, D. 1996. Model-based assessments of climate change effects on forests: a critical review. *Ecol Model* 90: 1–31.
- Miller, C. and Urban, D.L. 1999a. Fire, climate, and forest pattern in the Sierra Nevada, California. *Ecol Model* 114: 113–135.
- Miller, C. and Urban, D.L. 1999b. Forest pattern, fire, and climatic change in the Sierra Nevada. *Ecosystems* 2: 76–87.
- Miller, C. and Urban, D.L. 1999c. Interactions between forest heterogeneity and surface fire regimes in the southern Sierra Nevada. *Canadian J For Res* 29: 202–212.
- Minore, D. 1979. Comparative autecological characteristics of Northwestern tree species – a literature review. USDA GTR PNW 87. PNW Forest and Range Expt Station, Portland.
- Moore, I.D., Gryson, R.B. and Ladson, A.R. 1990. Digital terrain modelling: a review of hydrological, geomorphological, and biological applications. *Hydrol Processes* 5: 3–30.
- Mueller, M.J. 1982. Selected climatic data for a global set of standard stations for vegetation science. Junk, the Hague.
- Nikolov, N.T. and Zeller, K.F. 1992. A solar radiation algorithm for ecosystem dynamic models. *Ecol Model* 61: 149–168.
- Parton, W.J., Schimel, D.S., Cole, C.V. and Ojima, D. 1987. Analysis of factors controlling soil organic levels of grasslands in the Great Plains. *Soil Sci Soc Am J* 51: 1173–1179.
- Running, S.W. and Coughlan, J.C. 1988. A general model of forest ecosystem processes for regional applications. I. Hydrological balance, canopy gas exchange, and primary production processes. *Ecol Model* 42: 125–154.
- Running, S.W., Nemani, R.R. and Hungerford, R.D. 1987. Extrapolation of synoptic meteorological data in mountainous terrain and its use for simulating forest evapotranspiration and photosynthesis. *Can J For Res* 17: 472–483.
- Sellers, W.D. 1965. Physical climatology. University Chicago Press, Chicago.
- Shugart, H.H. 1984. A Theory of Forest Dynamics. Springer-Verlag, New York.
- Shugart, H.H., Smith, T.M. and Post, W.M. 1992. The potential for application of individual-based simulation models or assessing effects of climate change. *Ann Rev Ecol Syst* 23: 15–38.
- Smith, T.M. and Huston, M. 1989. A theory of the spatial and temporal dynamics of plant communities. *Vegetatio* 83: 49–69.
- Smith, T.M., Shugart, H.H., Bonan, G.B. and Smith, J.B. 1992. Modeling the potential response of vegetation to global climate change. *Adv Ecol Res* 22: 93–116.
- Solomon, A.M. 1986. Transient response of forests to CO₂-induced climate change: simulation modeling experiments in eastern North America. *Oecologia* 68: 567–579.
- Stephenson, N.L. 1988. Climatic control of vegetation distribution: the role of the water balance with examples from North America and Sequoia National Park, California. Ph.D. dissertation. Cornell University, Ithaca.
- Stephenson, N.L. 1990. Climatic control of vegetation distribution: the role of the water balance. *Am Nat* 135: 649–670.
- Stephenson, N.L. 1998. Actual evapotranspiration and deficit: biologically meaningful correlates of vegetation distribution across spatial scales. *J Biogeog* 25: 855–870.
- Stephenson, N.L. and Parsons, D.J. 1993. A research program for predicting the effects of climatic change on the Sierra Nevada. pp. 93–109. *In* Proceedings of the Fourth Conference on Research in California's National Parks. Edited by Veirs, S.D. Jr., Stohlgren, T.J. and Schonewald-Cox, C. U.S. Department of the Interior Park Service Transactions and Proceedings Series 9.
- Urban, D.L. Demographic process and gradient response in forested landscapes (in prep.).
- Urban, D.L., Acevedo, M.F. and Garman, S.L. 1999. Scaling fine-scale processes to large-scale patterns using models. pp. 70–98 *In* derived from models: meta-models. Spatial modeling of forest landscape change: approaches and applications. Edited by Mladenoff, D. and Baker, D. Cambridge University Press, Cambridge.
- Urban, D.L., Bonan, G.B. and Shugart, H.H. 1991. Spatial applications of gap models. *For Ecol Manag* 42: 95–110.
- Urban, D.L., Harmon, M.E. and Halpern, C.B. 1993. Potential response of Pacific Northwestern forests to climatic change: effects of stand age and initial composition. *Climatic Change* 23: 247–266.
- Urban, D.L., O'Neill, R.V. and Shugart, 1987. Landscape ecology *BioScience* 37: 119–127.
- Urban, D.L. and Shugart, H.H. 1992. Individual-based models of forest succession. pp 249–292 *In* Plant succession: theory and prediction. Edited by Glenn-Lewin, D.C., Peet, R.K. and Veblen, T.T. Chapman and Hall, London.
- Vankat, J.L. 1982. A gradient perspective on the vegetation of Sequoia National Park, California. *Madrono* 29: 200–214.
- VEMAP participants (J.M. Melillo and 26 others) 1995. Vegetation/ecosystem modeling and analysis project (VEMAP): comparing biogeography and biogeochemistry models in a continental-scale study of terrestrial ecosystem responses to climate change and CO₂ doubling. *Global Biogeochemical Cycles* 9: 407–437.
- Waring, R.H. and Schlesinger, W.H. 1985. Forest Ecosystems: Concepts and Management. Academic Press, Orlando.

- Waring, R.H., Schroeder, P.E. and Oren, R. 1982. Application of the pipe model theory to predict canopy leaf area. *Can J For Res* 12: 556–560.
- Watt, A.S. 1947. Pattern and process in the plant community *J Ecol* 35: 1–22.
- Weinstein, D.A. 1992. Use of simulation models evaluate the alteration of ecotones by global carbon dioxide increases. pp. 379–393. *Landscape Boundaries: Consequences for Biotic Diversity and Ecological Flows*. Edited by Hansen, A.J. and di Castri, F. Springer-Verlag, New York.
- Whittaker, R.H. and Woodwell, G.M. 1967. Surface area relations of woody plants and forest communities. *Am J Bot* 54: 931–939.
- Wiens, J.A. 1989. Spatial scaling in ecology. *Functional Ecol.* 8: 385–397.
- Wolock, D.M. and McCabe, G.J. 1995. Comparison of single and multiple flow direction algorithms for computing topographic parameters in TOPMODEL. *Water Resources Res* 31: 1315–1324.
- Yeakley, J.A., Swank, W.T., Swift, L.W., Hornberger, G.M. and Shugart, H.H. 1998. Soil moisture gradients and controls on a southern Appalachian hillslope from drought through recharge. *Hydrol Earth Syst Sci* 2: 41–49.
- Ziemer, R.R. 1964. Summer evapotranspiration trends as related to time after logging of forests in Sierra Nevada. *J Geophys Res* 69: 615–620.
- Zinke P.J. 1967. Forest interception studies in the United States. pp. 137–160. *In Forest Hydrology*. Edited by Sopper, W.E. and Lull, W. Pergamon, Oxford.